

THE SIZE OF SPANNING DISKS FOR POLYGONAL CURVES

JOEL HASS, JACK SNOEYINK, AND WILLIAM P. THURSTON

ABSTRACT. For each integer $n \geq 0$, there is a closed, unknotted, polygonal curve K_n in \mathbb{R}^3 having less than $10n + 9$ edges, with the property that any Piecewise-Linear triangulated disk spanning the curve contains at least 2^{n-1} triangles.

1. INTRODUCTION.

Let K be a closed polygonal curve in \mathbb{R}^3 consisting of n line segments. Assume that K is unknotted, so that it is the boundary of an embedded disk in \mathbb{R}^3 . This paper considers the question: How many triangles are needed to triangulate a Piecewise-Linear (PL) spanning disk of K ? The main result, Theorem 1 below, exhibits a family of unknotted polygons with n edges, $n \rightarrow \infty$, such that the minimal number of triangles needed in any triangulated spanning disk grows exponentially with n . More specifically, we construct a sequence of unknotted simple closed curves K_n in \mathbb{R}^3 having the following properties for each $n \geq 0$.

- The curve K_n is an unknotted polygon with at most $10n + 9$ edges.
- Any PL embedding of a triangulated disk into \mathbb{R}^3 with boundary K_n contains at least 2^{n-1} triangular faces.

The polygons K_1 and K_3 are pictured in Figure 1.

The existence of these curves is related to the complexity of certain topological algorithms. Algorithms to test knot triviality by a search for embedded PL spanning disks are searching for disks that can be exponentially more complicated than their boundary curves. Algorithms of this type include those described in [5],[3],[6],[9],[4]. Some approaches to problems in computational group theory, such as the word problem, are also based on a search for a spanning disk, and may face similar difficulties.

The lower bound given in our examples can be compared with the following upper bound: the results of [9] and [10] show that every unknotted polygon with at most n edges in \mathbb{R}^3 bounds a PL embedded triangulated disk which has at most Cn^2 triangles, where $C > 1$ is a constant independent of n . The exponent n^2 comes from the requirement that the polygon be embedded in the 1-skeleton of a triangulated 3-manifold. A triangulation that contains an n -edge polygon and using $O(n^2)$ tetrahedra always exists, and this bound cannot always be improved, see Avis and El Gindy [1]. On the other hand, [1] also shows that a set of points

Date: May 26, 2022.

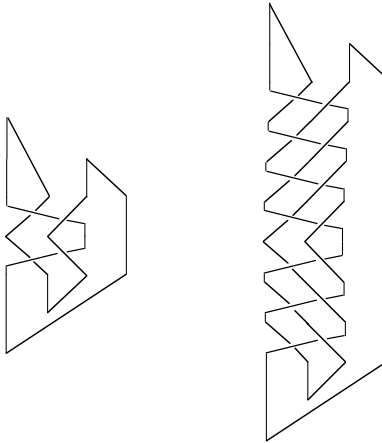
1991 Mathematics Subject Classification. Primary 57M25; Secondary 53A10.

Key words and phrases. knot theory, triangulations, combinatorial complexity, computational topology.

Partially supported by NSF grant DMS-0072348 and the Institute for Advanced Study.

Partially supported by grants from NSERC.

Partially supported by NSF grant DMS-0072540.

FIGURE 1. The curves K_1 and K_3 .

in general position, i.e. one for which no four points lie on a plane and no three on a line, can be triangulated using $O(n)$ simplices. It seems plausible that one could obtain an improved upper bound of C^n triangles for a PL spanning disk of a polygon whose vertices are in general position.

A result similar to the one proved in this paper was announced in [14], but the geometric analysis suggested there seems difficult to establish rigorously. We consider here a different set of polygonal curves K_n than those used in [14], and to establish their properties use topological arguments based on ideas from the classification of diffeomorphisms of surfaces [15] and from Morse theory [12].

Although the main result concerns PL curves and surfaces, in some parts of the proof it becomes convenient to work with smooth surfaces and smooth mappings. This allows use of basic results from smooth Morse theory. The arguments could be carried out entirely in the PL context, at the expense of using less well known versions of Morse theory. Passing between the PL and smooth settings is achieved by approximating PL maps by smooth maps.

2. CONSTRUCTION OF K_n

We now describe how to construct the unknotted curves K_n . The curve K_0 is contained in the xz -plane, see Figure 4. The construction of K_n begins with the PL 4-braid α depicted in Figure 2, where $\alpha = \sigma_1\sigma_2^{-1}$ in terms of the standard generators $\sigma_1, \sigma_2, \sigma_3$ of the braid group on four strands, see [2]. This braid consists of four arcs running between the planes $\{z = 1\}$ and $\{z = 0\}$, along each of which z is monotonically decreasing. The planes $\{z = 0\}, \{z = 1\}$ each intersect α at four points. We arrange these points along the x -axis and label them by $p_1 = (-2, 0)$, $p_2 = (-1, 0)$, $p_3 = (1, 0)$, $p_4 = (2, 0)$. In this labeling we only consider the xy -coordinates.

A diffeomorphism φ of the 4-punctured plane $\mathbb{R}^2 \setminus \{p_1, p_2, p_3, p_4\}$ is associated to the braid α . This diffeomorphism is induced by taking the punctured plane at level $z = 1$ and sliding it down the braid to level $z = 0$. Its action on the plane is indicated in Figure 3. The action is the identity outside a disk of radius three around the origin.

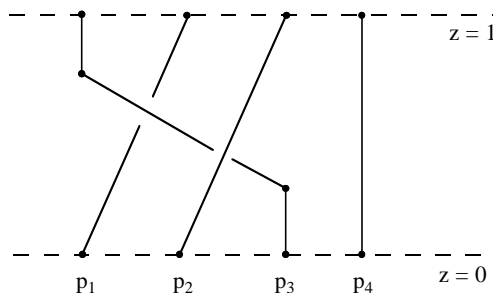


FIGURE 2. The braid α . The four arcs trace out the motion of p_1, p_2, p_3, p_4 under a continuous family of plane homeomorphisms beginning with the identity at $z = 1$ and ending with φ at $z = 0$. All the arcs lie in the xz -plane except the one running from p_1 to p_2 , which has two vertices off this plane.

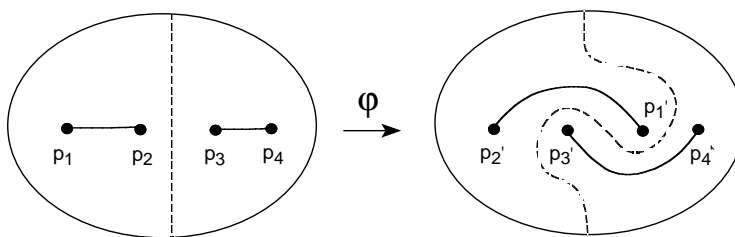


FIGURE 3. The diffeomorphism φ associated to α . The diffeomorphism is the identity outside a disk containing p_1, p_2, p_3, p_4 . The locations of the marked points remains fixed, $p'_2 = p_1, p'_3 = p_2$.

The curve K_n is formed from an iterated braid

$$\beta_n = \alpha^{-n} \circ \alpha^n,$$

running between the planes $\{z = n\}, \{z = -n\}$. Between each pair of planes $\{z = k\}$ and $\{z = k + 1\}$, K_n consists of a single copy of α for $0 \leq k \leq n - 1$ and a single copy of α^{-1} for $-n \leq k \leq -1$. In the braid group, β_n is equivalent to the trivial 4-braid, which consists of four parallel vertical segments. The construction of K_n is completed by appropriately connecting together the four strands at the upper and lower ends to form a closed curve, as shown in Figure 4. Above the plane $\{z = n\}$ we add a pair of line segments from p_1 at height $z = n + 2$ to each of p_1 and p_2 at height $z = n$, and from p_3 at height $z = n + 1$ to each of p_3 and p_4 at height $z = n$. Similarly, below the plane $\{z = -n\}$ we add a pair of line segments from p_2 at height $z = -n - 1$ to each of p_2 and p_3 at height $z = -n$, and from p_2 at height $z = -n - 2$ to each of p_1 and p_4 at height $z = -n$. Because the braids α^n and α^{-n} cancel in the braid group, it is clear that K_n is unknotted.

Our main result is the following:

Theorem 1. For each $n \geq 0$,

1. K_n is unknotted.

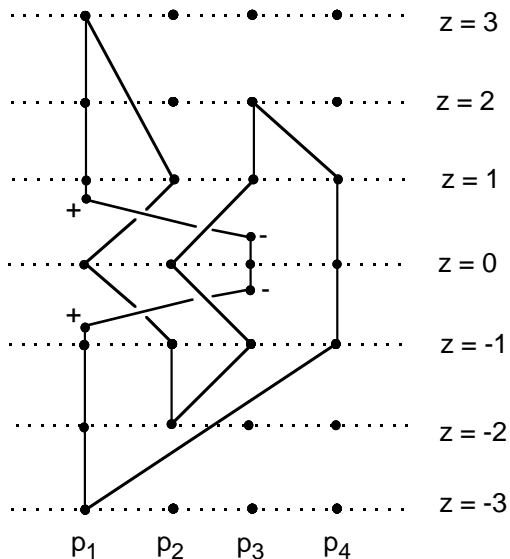


FIGURE 4. A closer look at the unknot K_1 . All segments lie in the xz -plane except three segments from p_1 to p_3 between $z = 1$ and $z = 0$ and three segments from p_3 to p_1 between $z = 0$ and $z = -1$. These have y coordinates above and below the xz -plane, as indicated by the $+$ and $-$ symbols.

2. K_n contains at most $10n + 9$ edges.
3. Any piecewise-smooth embedded disk spanning K_n intersects the y -axis in at least 2^{n-1} points.
4. Any embedded PL triangulated disk D_n bounded by K_n contains at least 2^{n-1} triangles.

The condition (3) that the disk intersects a line many times implies condition (4), that it contains many triangles, since each triangle can intersect a line transversely at most once.

We prove Theorem 1 in §3. We first construct a *standard spanning disk* for K_n , which we call F_n . Figure 6 shows F_0 and F_1 . To understand the behavior of F_n and other disks spanning K_n , we prove some facts about diffeomorphisms and “train tracks”. These are applied in §4 to count the intersections of the y -axis and F_n . In §5 we use Morse Theory to show that any other spanning disk is at least as complicated, along the y -axis, as the standard disk.

3. CONSTRUCTION OF A STANDARD SPANNING DISK

In this section we describe how to construct for each K_n a particular smooth spanning disk F_n . This *standard disk* intersects each plane $\{z = c\}$, $-n - 1 < c < n + 1$ in two arcs, which are embedded and disjoint. At $z = \pm n$ the arcs lie along the x -axis, joining p_1, p_2 and p_3, p_4 respectively. For $n \geq 2$ these arcs are shown in Figure 5 at heights $z = n, z = n - 1$ and $z = n - 2$. In Figure 5 the four arcs appear in the three pictures in order $(1, 2, 3, 4)$, $(2, 3, 1, 4)$ and $(3, 1, 2, 4)$, read left to right.

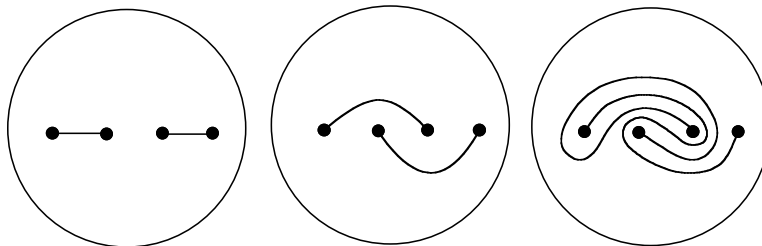


FIGURE 5. Arcs of intersection of a standard disk with the planes $\{z = n\}$, $\{z = n - 1\}$ and $\{z = n - 2\}$.

Above the plane $\{z = n\}$ the standard disk consists of two triangles in the xz -plane, one with a base along the segment from p_1 to p_2 and one with a base along the segment from p_3 to p_4 . Below $z = -n$ it is bounded by a six-sided polygon in the xz -plane meeting $\{z = n\}$ along two segments, one running from p_1 to p_2 and one from p_3 to p_4 . Between $\{z = n\}$ and $\{z = -n\}$ the standard disk twists so that its boundary follows K_n , as made precise below.

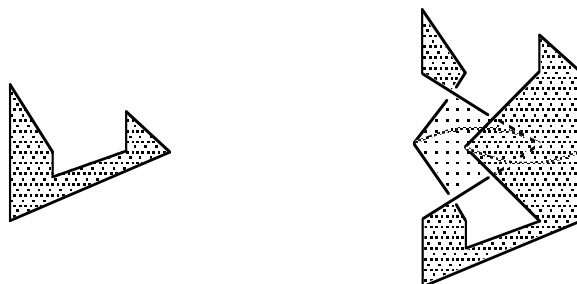


FIGURE 6. The standard disks F_0 and F_1 .

The arcs in the first disk of Figure 5 are taken by φ to the arcs in the second disk in the Figure, and those in turn are taken by φ to the arcs in the rightmost disk. The arcs of the braid indicate the motion of the disk in the process of sliding from $z = 1$ to $z = 0$. A composition of a counterclockwise half-twist interchanging the first two punctures, followed by a clockwise half-twist interchanging the second two punctures gives φ . Corresponding to the braid α^n is the iterate φ^n of φ .

We now give a precise description of the construction of F_n , based on φ . Begin with a planar polygonal curve bounding a disk L_n in the xz -plane, formed as follows: Take vertical segments from $(-2, 0, -n)$ to $(-2, 0, n)$, $(-1, 0, -n)$ to $(-1, 0, n)$, $(1, 0, -n)$ to $(1, 0, n)$ and $(2, 0, -n)$ to $(2, 0, n)$. At the top, add a line segment from $(-2, 0, n+2)$ to each of $(-2, 0, n)$, $(-1, 0, n)$ and from $(1, 0, n+1)$ to each of $(1, 0, n)$, $(2, 0, n)$. At the lower end, add a line segment connecting $(-2, 0, -n-2)$ to each of $(-2, 0, -n)$, $(2, 0, -n)$ and $(-1, 0, -n-1)$ to each of $(-1, 0, -n)$, $(1, 0, -n)$, as shown in Figure 7.

The standard disk F_n is the image of this planar disk L_n under a diffeomorphism $J_n : \mathbb{R}^3 \rightarrow \mathbb{R}^3$, that preserves the z -coordinates of points, and carries the boundary of L_n to K_n . The diffeomorphism φ is isotopic to the identity map on the plane. So there is a continuous family of diffeomorphisms of the plane φ_t , $0 \leq t \leq 1$,

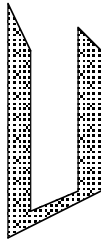


FIGURE 7. A planar disk L_n , lying between $\{z = n + 2\}$ and $\{z = -n - 2\}$, is twisted to form F_n .

with $\varphi_1 = \text{identity}$ and $\varphi_0 = \varphi$. Define a diffeomorphism $G : \mathbb{R}^2 \times [0, 1] \rightarrow \mathbb{R}^2 \times [0, 1]$ by $G(x, y, t) = (\varphi_t(x, y), t)$. Then G carries the vertical line segments in $\mathbb{R}^2 \times [0, 1]$ with xy -coordinates $(-2, 0), (-1, 0), (1, 0), (2, 0)$ to the braid α . Also define a diffeomorphism $H : \mathbb{R}^2 \times [0, 1] \rightarrow \mathbb{R}^2 \times [0, 1]$, by $H(x, y, t) = (\varphi(x, y), t)$. This extends φ to $\mathbb{R}^2 \times [0, 1]$ as a product. The diffeomorphism J_n is defined to be the identity for $z \geq n$ and $z \leq -n$. For $0 \leq k \leq t \leq k + 1 \leq n$, $J_n(x, y, t) = G \circ H^{n-k-1}(x, y, t - k) + (0, 0, k)$, and for $-n \leq k - 1 \leq t \leq k \leq 0$, $J_n(x, y, t) = G \circ H^{n+k-1}(x, y, k - t) + (0, 0, 2t - k)$.

A Morse function f on a smooth closed manifold has a finite number of critical points $\{c_i\}$ with distinct values under f . A Morse function on a manifold with boundary is a Morse function when restricted to both the boundary and the interior of the manifold. Critical points are either interior critical points or boundary critical points. A Morse function on a disk has at least two critical points, one maximum and one minimum, and if there are exactly two critical points then both must occur on the boundary, since there is a maximum and minimum value for the restriction to the boundary. The construction of F_n gives z as a Morse function on F_n that has four critical points. Two are maxima, at $z = n + 2$ and $z = n + 1$, one is a minimum, at $z = -n - 2$, and one is a saddle point, at $z = -n - 1$. All four critical points lie on the boundary of F_n .

4. AN INVARIANT TRAIN TRACK FOR φ

To understand the iterates of φ , we use an associated combinatorial object called an *invariant train track*. The theory of train tracks is described in [15]; we need here only elementary ideas from this theory. A *train track* is a 3-valent graph that is embedded on a surface. The edges, called *tracks*, are embedded smoothly and the three tangent directions at the vertices, called *switches*, lining up to give a C^1 -embedding of the union of any pair of edges meeting at a vertex. Train tracks have *fibered neighborhoods*, closed neighborhoods filled by fibers. Fibers are intervals transverse to the edges, much like the tracks of a mono rail, and there is a projection map of the fibered neighborhood to the train track. A curve is *carried* by a train track if it can be isotoped into the fibered neighborhood so that it is transverse to the fibers. Such a curve is roughly parallel to the tracks, but may run many times over each track. The curve is determined up to isotopy by a set of *weights*. These are non-negative integers assigned to each track, giving the number of times the curve runs over that edge, in either direction. At each switch there is a *switching condition*: the weight assigned to the one “incoming” track is the sum

of the weights of the two “outgoing” tracks. The weights for any two tracks near a vertex determine the weight for the third. An example is shown in Figure 8.

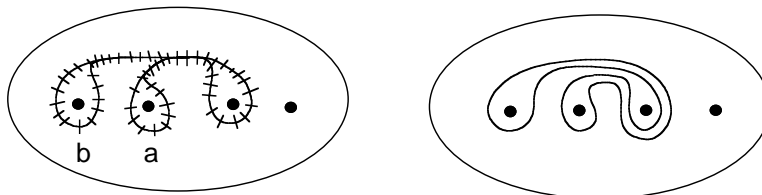


FIGURE 8. A train track T , showing its fibered neighborhood, and a curve that it carries with weights $a = 1$ and $b = 1$. Other weights are determined by the switching conditions.

A curve C carried by a train track can be *projected* onto the train track, meaning that the embedding of the curve can be composed with the projection of each fiber in the fibered neighborhood to the base point of that fiber on the train track. Each track is given a weight by the projection, corresponding to the number of pre-images in C of a point in the interior of the track. The curve C can be reconstructed from these weights, by taking a number of copies of each track given by the weights and joining them together near the switches. There is a unique way to join that gives an embedded curve. The resulting simple closed curve is unique up to isotopy.

As with curves, a train track T' is *carried* by another train track T if T' can be isotoped into a fibered neighborhood of T so that its vertices are carried to vertices and so that the tracks of T' are transverse to the fibers of the fibered neighborhood of T . We can then *project* T' into T by mapping each fiber to its base point on T . If T' carries weights on its branches, then these can be summed to give weights on the branches of T to which it projects, as in Figure 9.

A train track is said to be *invariant* under a diffeomorphism φ of a surface if its image $\varphi(T)$ is carried by T .

For later application, we replace the level planes $\{z = c\}$ of the height function z with the level sets of a different function $f_n : \mathbb{R}^3 \rightarrow \mathbb{R}$, that agrees with z in a large ball around the origin, a ball that contains the disks we will be considering. Thus in subsequent arguments we will be able to view either f_n or z interchangeably as the Morse function we are using. The level sets of f_n are a family of spheres rather than planes $\{z = c\}$. To construct f_n , we first choose a large constant $R_n > 0$ such that a ball of radius R_n centered at the origin contains F_n in its interior. For each t with $-R_n < t < R_n$, define Σ_t to be the 2-sphere obtained by taking the disk $\{(x, y, z) : x^2 + y^2 \leq R_n, z = t\}$ and capping it to form a convex 2-sphere enclosing the point $(0, 0, -2R_n)$. Figure 10 shows some of these spheres. The spheres are the level sets of a function

$$f_n : \mathbb{R}^3 \rightarrow [-2R_n, \infty).$$

The restriction of f_n to the disks we will consider agrees with z , and R_n will be chosen large enough so that the level sets of f_n look identical to flat planes in a ball containing the disks. Note that we can use different functions f_n for different values of n , if necessary, to ensure that our choice of R_n is sufficiently large. The diffeomorphism of the 4-punctured plane φ , which was the identity outside of a

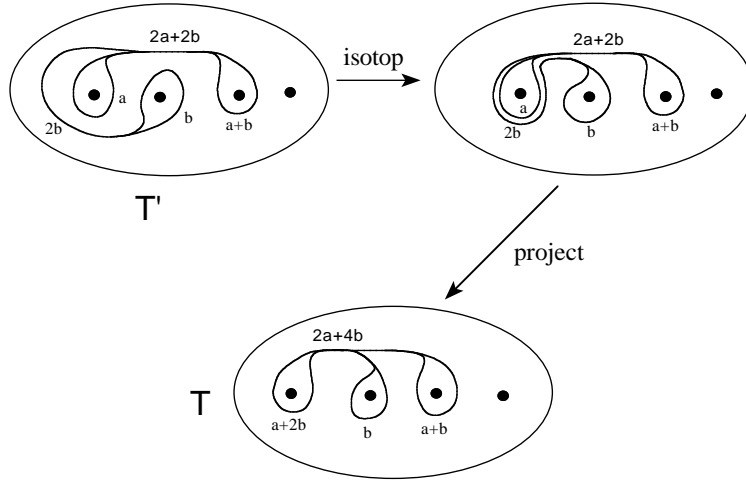


FIGURE 9. A train track T' is projected into another train track T' that carries it. The weights of the tracks on T' that project to a given track on T are summed to give weights on that track.

disk of radius three around the origin, induces a diffeomorphism $\varphi : S \rightarrow S$ of the 4-punctured sphere S , which we call by the same name.

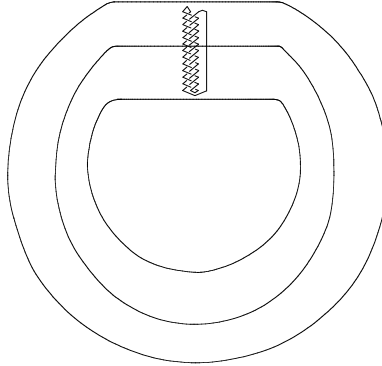


FIGURE 10. Level sets of the function f_n are spheres, but in a ball containing K_n the level sets are the same as those of the z coordinate.

There is an invariant train track T for φ , depicted in Figure 11, and also shown with a fibered neighborhood in Figure 8. An assignment of weights to all the tracks of T is completely determined by assigning two weights a and b on the two indicated tracks, as in Figure 8. The non-negative integers a and b are arbitrary, but all other weights are determined by the switching conditions. Each choice of a, b gives rise to a unique simple closed curve carried by T , and we refer to a, b as the weights with which this curve is carried by T .

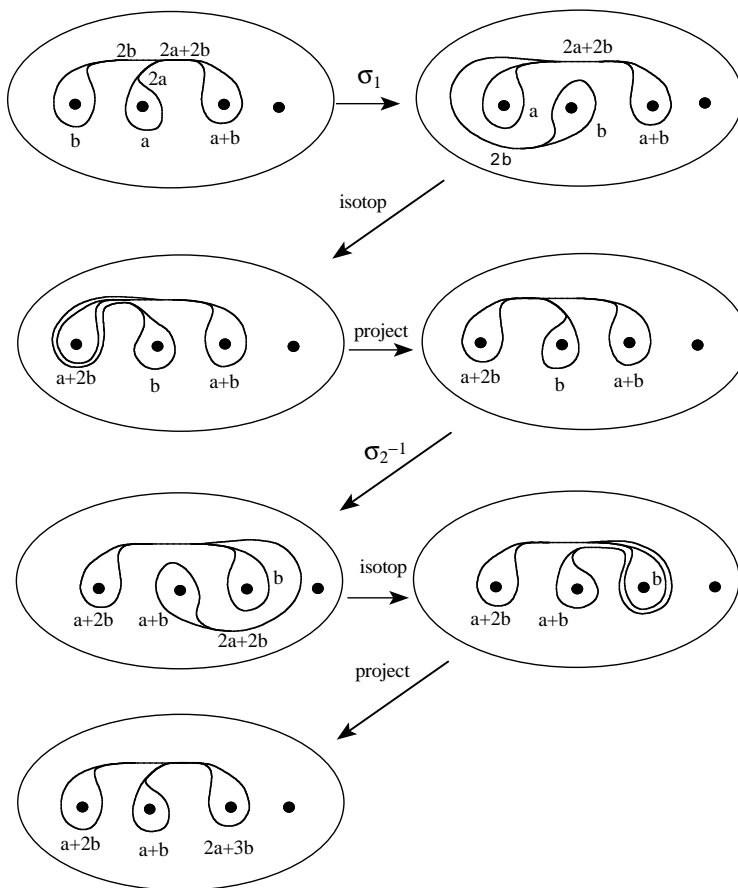


FIGURE 11. An invariant train track T for φ . Here σ_1 and σ_2^{-1} denote diffeomorphisms of the four punctured disks associated to the braid group elements σ_1 and σ_2^{-1} . The composition of these two diffeomorphisms gives φ , showing that T is invariant under φ .

To understand the iterates of φ we study the image of T under φ . The image $\varphi(T)$ can be isotoped so that vertices of $\varphi(T)$ go to vertices of T and tracks of $\varphi(T)$ are transverse to the fibers of the fibered neighborhood of T , as indicated in Figure 11.

Lemma 2. *The train track T is invariant under the homeomorphism φ . A curve carried by T with weights a, b is mapped by φ to a curve carried by T with weights $a + b$ and $a + 2b$.*

Proof: The image of T under φ can be isotoped into the fibered neighborhood of T as shown in Figure 11. The tracks with initial weights a and b have projected onto them tracks with total weight $a + b$ and $a + 2b$ respectively. A curve carried by T with weights a, b is similarly carried to a curve carried with weights $a + b, a + 2b$. \square

So T is an invariant train track for φ , and a curve C carried by T with weights a and b , has image $\varphi(C)$ which is also carried by T , but with weights $a + b$ and $a + 2b$. When φ is iterated, the weights on these two tracks grow according to a Fibonacci sequence:

$$\{(a, b), (a + b, a + 2b), (2a + 3b, 3a + 5b), (5a + 8b, 8a + 11b), \dots\}.$$

Lemma 3. *A curve carried by T with weights $a_0 \geq 0$ and $b_0 \geq a_0$ is mapped by the diffeomorphism φ^n to a curve carried by T with weights a_n and b_n , satisfying $a_n \geq 2^n a_0$ and $b_n \geq 2^n b_0$.*

Proof: Under the action of φ the weight a corresponding to a curve C is transformed to the weight $a + b \geq 2a$ corresponding to $\varphi(C)$ and the weight b to $a + 2b \geq 2b$. The result follows by iterating n times. \square

Let B denote the simple closed curve on a 4-punctured sphere S that separates the points p_1, p_2 from p_3, p_4 , as shown in Figure 12. We analyze the number of intersections between B and a curve C in the 4-punctured sphere S that is carried by T with weights a, b . We show there is no isotopy of C in the 4-punctured sphere which can reduce the number of intersections with B below $2a + 2b$.

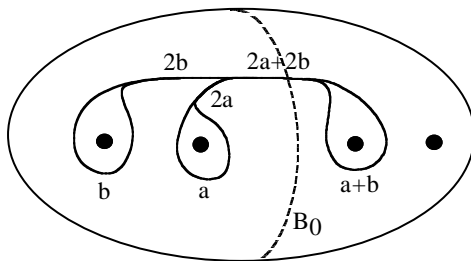


FIGURE 12. The curve B intersects a curve carried by the train track T in at least $2a + 2b$ points.

Lemma 4. *A curve C in S that is carried by the train track T with weights a and b intersects B in at least $2a + 2b$ points.*

Proof: In a surface containing two intersecting simple closed curves, a *2-gon* is a disk on the surface whose boundary consists of an arc from each of the curves and whose interior is disjoint from each of them. It is shown in [11, Lemma 3.1, pp. 108] that if two simple closed curves on a surface have more intersections than the minimal possible number in their isotopy class, then each contains an arc such that the two arcs together bound a 2-gon on the surface.

Let C be a curve lying in the fibered neighborhood of T , transverse to the fibers and carried with weights a and b . It follows from the above that if C can be isotoped in S to have fewer than $2a + 2b$ points of intersection with B , then there exists an arc β contained in B and an arc γ contained in C that together bound a 2-gon in S , whose interior is disjoint from $B \cup C$. We will show that there is no such 2-gon between C and B , and hence that C can not be isotoped to reduce the number of its intersections with B .

The arc γ lies on C and so lies in the fibered neighborhood of T , and is transverse to the fibers. Moreover γ intersects B only at its two endpoints, and therefore lies

either to the right or to the left of B on S , where “left” refers to the side containing p_1, p_2 and “right” to the side containing p_3, p_4 .

An arc carried by T with interior to the right of B runs once around the third puncture and, together with β , must separate the third and fourth punctures. Similarly an arc carried by T with interior on the left of B runs once around either the first or second punctures before returning to B , and together with β separates the first and second punctures. In either case such an arc is not homotopic to an arc in B , (rel boundary), and therefore cannot cobound a disk with an arc β contained in B . So $\beta \cup \gamma$ cannot cobound a 2-gon, and it follows that the number of intersections of B and C cannot be reduced. \square

Corollary 5. *Let p_1, p_2, p_3, p_4 denote four distinct marked points on a 2-sphere and let B denote a simple closed curve separating p_1, p_2 from p_3, p_4 . Let δ be the simple closed curve that is the boundary of a neighborhood of an arc joining p_1 to p_2 in the complement of B . Then $\varphi^n(\delta)$ intersects B in at least 2^n points.*

Proof: While δ is not carried by T , its image $\varphi(\delta)$ is carried by T with weights $a = 0, b = 1$, and $\varphi^2(\delta)$ is carried with weights $a = 1, b = 2$. Lemma 3 can be applied to $\varphi^2(\delta)$ and its iterates, so $\varphi^n(\delta) = \varphi^{n-2}\varphi^2(\delta)$ is carried with weights at least $a = 2^{n-2}, b = 2^{n-1}$. By Lemma 4, the curve B intersects a curve carried by the train track with weights a, b in at least $2a + 2b$ points. Since $2a + 2b \geq 2b \geq 2^n$, the result follows. \square

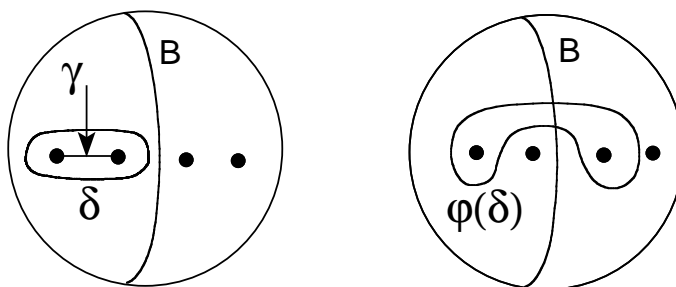


FIGURE 13. The curves γ, δ and $\varphi(\delta)$ on a sphere with four marked points removed.

Corollary 6. *An arc γ joining p_1 to p_2 in the complement of B has image under φ^n that intersects the closed curve B on the 4-punctured 2-sphere S in at least 2^{n-1} points.*

Proof: The simple closed curve δ is isotopic to the boundary of a regular neighborhood of γ and $\varphi^n(\delta)$ is isotopic to the boundary of a regular neighborhood of $\varphi^n(\gamma)$. For any arc in S that intersects B transversely, the boundary of a sufficiently thin neighborhood of the arc intersects B in twice the number of points that the arc intersects B . If $\varphi^n(\gamma)$ intersected B in fewer than 2^{n-1} points then we can form a thin neighborhood of $\varphi^n(\gamma)$ whose boundary intersects B in less than 2^n points, contradicting Corollary 5. \square

5. COMBINATORIAL COMPLEXITY OF SPANNING DISKS FOR K_n

In this section we show that any PL spanning disk for K_n contains exponentially many triangles, proving the main result.

Proof of Theorem 1: Let n be any fixed positive integer. The assertion (1) that K_n is unknotted follows from its construction as the composition of a braid and its inverse.

The curve K_n can be constructed with straight segments as follows: Four segments above $\{z = n\}$ and four below $\{z = -n\}$ cap off the braid. Between $\{z = n\}$ and $\{z = -n\}$, a single line segment forms the entire fourth strand, and the first three strands are formed from $2n$ copies of the first three strands of α . Each copy of α requires five segments for the first three strands. The total number of segments needed is no more than $10n + 9$, which is assertion (2).

We prove assertion (3) in three steps. Recall that for each fixed n , K_n bounds a smooth disk F_n in \mathbb{R}^3 that we call the standard disk, and that $B_0 = \Sigma_0 \cap \{x = 0\}$ is the closed curve obtained by intersecting Σ_0 with the plane $\{x = 0\}$. We first show that B_0 intersects F_n in at least 2^{n-1} points. We then consider an arbitrary smooth spanning disk E_n , and show that the number of intersections of E_n with B_0 is at least as large as that of F_n with B_0 . In the third step, we approximate an arbitrary PL disk D_n by a smooth disk to obtain the same conclusion in the PL setting.

The standard disk F_n is swept out by arcs joining points of K_n in the level sets $\{z = \text{constant}\}$, as they descend from $\{z > n + 2\}$ to $\{z < -n - 2\}$. One arc appears below $\{z = n + 2\}$, the second below $\{z = n + 1\}$. The arcs join together to form a single arc at $\{z = -n - 1\}$, and this in turn disappears below $\{z = -n - 2\}$. The height function given by the restriction of the z -coordinate to F_n defines a Morse function on F_n , and this Morse function has no critical points in the interior of F_n .

The arc $\gamma = \gamma_n$ in $F_n \cap \{z = n\}$ connects p_1 and p_2 , as shown in Figure 13. Denote by γ_t the arc in $F_n \cap \{z = t\}$ that is in the same component of $F_n \cap \{z \geq t\}$ as γ . For each integer k with $0 < k \leq n$, as we slide γ_k down one unit along F_n , γ_k is deformed along F_n to $\gamma_{k-1} = \varphi(\gamma_k)$. So as t decreases to 0, the arc γ_n is slid along F_n to an arc γ_0 that is the image of n iterations of φ .

Let B_0 denote the closed curve along which the level set $\Sigma_0 = f_n^{-1}(0)$ intersects the yz -plane. Then B_0 separates the four points of intersection of Σ_0 and K_n into pairs, p_1, p_2 and p_3, p_4 . The standard disk F_n intersects B_0 in at least 2^{n-1} points by Corollary 6.

Our goal is to show that an arbitrary PL disk bounded by K_n intersects B_0 in at least as many points as does F_n . Before considering PL disks, we first consider a smooth spanning disk E_n . In this setting we will apply some basic results from the Morse Theory of smooth functions on surfaces; see [12] for an exposition of smooth Morse Theory. We will then shift back to the PL setting. The height function z , or the function f_n that agrees with it on the region we are studying, will serve as the Morse functions. Let E_n denote an arbitrary disk spanning K_n such that

1. E_n has smoothly embedded interior.
2. The height function z restricted to E_n is a Morse function.

We now show, using Morse theory, that the surface E_n intersects the closed curve B_0 in at least as many points as does the ‘‘standard disk’’ F_n . Choose a value of R_n large enough so that F_n and E_n both lie in the interior of the ball of radius

R_n , and as before form the Morse function f_n whose level sets are spheres Σ_t for $t > -2R_n$. The intersection of E_n with the spheres Σ_t at non-critical levels is contained in $\Sigma_t \cap \{z = t\}$. As t decreases from ∞ to $-2R_n$, the sphere Σ_t begins to intersect $K_n = \partial E_n$, when $t = n + 2$. As t decreases there are first one, then two arcs in $\Sigma_t \cap E_n$, along with a (possibly empty) collection of simple closed curves. For $n + 1 < t < n + 2$, $\Sigma_t \cap E_n$ consists of a single arc β_t , along with a possibly empty collection of simple closed curves. For $-n < t < n$, $\Sigma_t \cap E_n$ contains two arcs connecting the four points of $\Sigma_t \cap K_n$. As t decreases from $n + 1$, β_t is continuously deformed as long as E_n is transverse to Σ_t . As long as the transversality continues to hold, let β_t denote the arc that is in the same component of $E_n \cap \{z \geq t\}$ as β .

As long as passing through the critical level $\{t = c\}$ does not change which pairs of points on K_n are connected by the pairs of arcs, it is possible to extend the definition of β_t to one of the two arcs below the critical point. We define $\beta_{c-\epsilon}$ to be the arc connecting the same pair of points as $\beta_{c+\epsilon}$. In these cases even the isotopy class of the arc is preserved, though the curve β_t does not change continuously when t passes through the critical level c .

For the values $-n < t < n$, the level sets of f_n are transverse to K_n , so any critical points lie in the interior of the disk E_n . There are three types of changes in β_t that can occur when descending from $\Sigma_{c+\epsilon}$ to $\Sigma_{c-\epsilon}$, as indicated in Figure 14.

1. Moving past a saddle critical point connects $\beta_{c+\epsilon}$ to a simple closed curve of $\Sigma_{c+\epsilon} \cap E_n$ to form $\beta_{c-\epsilon}$.
2. Moving past a saddle critical point connects $\beta_{c+\epsilon}$ to itself to form $\beta_{c-\epsilon}$ together with a simple closed curve.
3. Moving past a saddle critical point connects $\beta_{c+\epsilon}$ to the second arc of $\Sigma_{c+\epsilon} \cap E_n$. No arc $\beta_{c-\epsilon}$ is defined.

The first two types of moves are inverses, since reversing the direction of a type (1) move gives a type (2) move and vice-versa. The level surface in which $\beta_{c+\epsilon}$ lies is either a 2-punctured sphere, if $c \geq n + 1$ or $c \leq -n - 1$, and is a 4-punctured sphere otherwise. In a 2-punctured sphere there is a unique isotopy class of arcs connecting the two punctures, so the isotopy class of β_t in Σ_t is unchanged when passing through the critical point. In a 4-punctured sphere there are many isotopy classes of arcs connecting two of the punctures, but as we pass a saddle critical point of type (1) or type (2), the curve β_t remains in the complement of the second arc of intersection. The complement of an arc in a sphere is homeomorphic to an (open) disk, and in a disk there is a unique isotopy class of arcs connecting any two points. So the isotopy class of β_t in Σ_t remains unchanged by a saddle move in these cases.

The third type of critical point does change the isotopy class of the arc, since it changes the boundary points connected by the arc. The following lemma asserts that this can occur at most once.

Lemma 7. *Suppose that $f_n : D \rightarrow \mathbb{R}$ is a Morse function on a topological disk D that restricts to a Morse function on ∂D . Suppose also that $f_n|_{\partial D}$, the restriction of f_n to ∂D , has at most four critical points on ∂D . Then f_n can have at most one interior critical point of type (3) that is a saddle connecting distinct arcs in the level set of f_n .*

Proof: Suppose there is an interior critical point with critical value c that is a saddle connecting distinct arcs in the level set $f_n = c + \epsilon$. The four arcs leaving the saddle point hit the boundary of D at four distinct points. These arcs divide

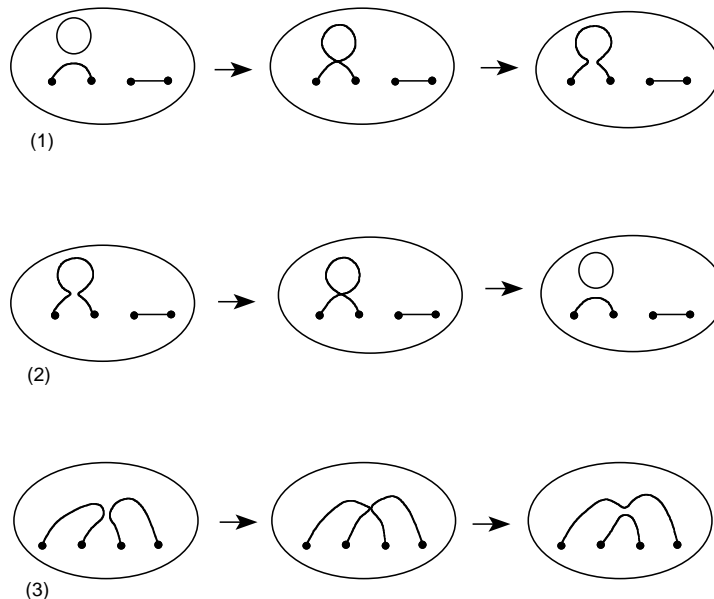


FIGURE 14. Three types of changes can occur in the level sets $E_n \cap \{z = t\}$ as they pass through a critical point.

D into four quadrants, which meet ∂D in four arcs. Each of the boundary arcs has its two endpoints on the level set $f_n = c$, and is non-constant on these boundary arcs. So each contains at least one maximum or minimum of $f_n|_{\partial D}$. Suppose there were a second saddle critical point on a level set $\{f_n = c'\}$. Since critical points of Morse functions have distinct values, we have that $c' \neq c$. The four arcs emerging from the second saddle are therefore disjoint from the first critical level set, and contained in one of the previously defined quadrants. See Figure 15.

The intersection of this quadrant with ∂D has four points on which f_n takes the value c' , and therefore $f_n|_{\partial D}$ has at least three critical points in this quadrant. It follows that $f_n|_{\partial D}$ has at least six critical points, contradicting the hypothesis. So only one saddle of type (3) can occur. \square

Since E_n is a topological disk whose boundary has four critical points for the height function, at most one type (3) critical point can occur. Assume first that a type (3) critical point does not occur for $t > 0$. On the standard disk, γ_0 is obtained from γ_n by a continuous deformation involving no critical points, while β_0 is obtained from β_n by a process that may include passing through critical points of types (1) and (2), but none of type (3). Therefore the isotopy class of β_0 in the 4-punctured sphere is the same as that of $\beta_{n+2-\epsilon}$. Since β_t is isotopic to γ_t for t close to $n+2$, we conclude that β_0 is isotopic to γ_0 . By Lemma 4 β_0 intersects B_0 in at least as many points as γ_0 .

Now consider the case where a type (3) critical point does occur for some $t > 0$. By Lemma 7, there are no type (3) critical points for $t < 0$. In this case we repeat the previous argument, but using the function $-f_n$ rather than f_n . Note that as z increases from $\{z = k\}$ to $\{z = k+1\}$ for k an integer with $-n \leq k \leq -1$, the level sets of F_n are again transformed by an application of φ . We replace γ with the

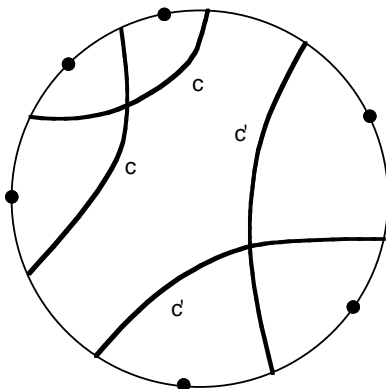


FIGURE 15. The existence of two type (3) saddle critical points on a disk, at levels $f_n^{-1}(c)$ and $f_n^{-1}(c')$, imply that the boundary of the disk has at least six critical points.

arc γ' in $E_n \cap \Sigma_{-n}$ which joins p_2 to p_3 , and δ with δ' , the boundary of a regular neighborhood of γ'_n .

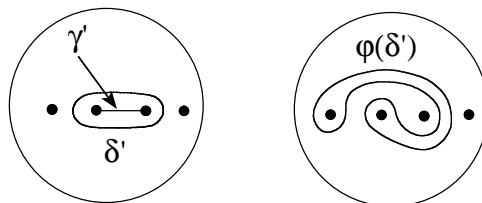


FIGURE 16. The curves γ' , δ' and $\varphi(\delta')$.

The curve δ' is carried with weights $a = 1, b = 0$ by T and $\varphi(\delta')$ is carried with weights $a = 1, b = 1$. By Lemma 3, $\varphi^n(\delta')$ is carried by T with weights $a \geq 2^{n-1}$ and $b \geq 2^{n-1}$. By Lemma 4 a curve isotopic to $\varphi^n(\delta')$ intersects B_0 in at least $2a + 2b = 2^{n+1}$ points. Then $\varphi^n(\gamma')$ intersects B_0 in at least half as many, or 2^n points. As t increases from $-n$ to 0 , the arc γ'_t in the component of $E_n \cap \{z \leq t\}$ containing γ' , is carried to an arc in Σ_0 isotopic to $\varphi^n(\gamma'_n)$. So E_n again must intersect B_0 in at least 2^{n-1} points. In every case the curve B_0 intersects E_n in at least 2^{n-1} points.

Now consider an arbitrary PL disk D_n with boundary K_n . After an arbitrarily small isometry of \mathbb{R}^3 , we can arrange that D_n intersects the y -axis transversely in a finite number of points, The disk D_n can be approximated by a disk E_n , with smoothly embedded interior, that coincides with D_n in a neighborhood of each intersection point with the y -axis, and that remains disjoint from other points of the y -axis. We choose R_n larger, if necessary, so that in the passage from the Morse function z to the Morse function f_n , the three surfaces D_n, E_n and F_n that we consider only intersect the flat parts of the spheres S_t which form the level sets of f_n . So the intersection of B_0 with D_n, E_n and F_n is the same as that of the

y -axis with these surfaces, each intersection being in the interior of a triangular face of D_n .

But we have shown that E_n intersects B_0 in at least 2^{n-1} points, and it therefore follows that the PL disk D_n also intersects B_0 in at least 2^{n-1} points.

Since a triangle transversely intersects a line in at most one point, and B_0 agrees with the y -axis in a ball containing D_n , E_n and F_n , this implies that D_n contains at least 2^{n-1} triangles, and Theorem 1 is proved. \square

Remarks:

1. If we allow spanning disks that self-intersect, then the number of triangles required to span K_n grows only linearly with n . If a spanning surface of arbitrary genus is allowed, it can be shown that the number of triangles required to span K_n grows at most quadratically in n [7].
2. The number of Reidemeister moves required to transform any unknotted curve constructed with n polygonal edges into a single triangle has an exponential upper bound derived in [6]. For the particular K_n constructed here, the number of Reidemeister moves required to transform the projection of K_n to a projection with no crossings grows only linearly with n .
3. The argument establishes somewhat better estimates than claimed above. If we embed K_n into \mathbb{R}^3 in a more efficient way, then for large n , K_n has at most $6n$ segments and the number of triangles contained in any disk spanning K_n grows faster than a constant times ϕ^{2n} , where ϕ is the golden ratio.

6. ACKNOWLEDGMENTS

This paper was completed while the first author was visiting the Institute for Advanced Study. The authors are grateful to J. Lagarias and the referee for helpful suggestions on the exposition.

REFERENCES

- [1] D. Avis and H. El-Gindy, *Triangulating point sets in space*, Discrete Comput. Geom. 2 (1987), no. 2, 99–111.
- [2] J. Birman, *Braids, Knots and the Mapping Class Group*, Princeton University Lecture Notes.
- [3] J. Birman and M.D. Hirsch, *Recognizing the unknot*, Geom. Topol. 2 (1998), 175–220 (electronic).
- [4] S. Galatolo, *On a problem in effective knot theory*, Atti Accad. Naz. Lincei Cl. Sci. Fis. Mat. Natur. Rend. Lincei (9) Mat. Appl. 9 (1998), no. 4, 299–306 (1999).
- [5] W. Haken, *Theorie der Normalflächen, ein Isotopie Kriterium für ein Kreis*, Acta Math., **105** (1961), 245–375.
- [6] J. Hass and J. C. Lagarias, *The number of Reidemeister moves needed for unknotting*, J. Amer. Math. Soc. 14 (2001), 399–428.
- [7] J. Hass and J. C. Lagarias *Combinatorial isoperimetric inequalities in \mathbb{R}^d* . In preparation.
- [8] J. Hass, J. C. Lagarias and N. Pippenger, *The computational complexity of knot and link problems*, preliminary report, Proc. 38th Annual Symposium on Foundations of Computer Science, (1997) 172–181.
- [9] J. Hass, J. C. Lagarias and N. Pippenger, *The computational complexity of knot and link problems*, J. ACM 46 (1999), no. 2, 185–211.
- [10] J. Hass, J. C. Lagarias and W.P. Thurston, *Area Inequalities for Embedded Disks Bounding Unknotted Curves*, in preparation.
- [11] J. Hass and G.P. Scott, *Intersections of curves on surfaces*, Israel J. Math. 51 (1985), no. 1-2, 90–120.
- [12] J. Milnor, *Morse theory*, Annals of Mathematics Studies, No. 51 Princeton University Press, Princeton, N.J. 1963.

- [13] R.C. Penner and J.L. Harer, *Combinatorics of train tracks*, Annals of Mathematics Studies, 125. Princeton University Press, Princeton, NJ, 1992.
- [14] J. Snoeyink, A trivial knot whose spanning disks have exponential size, Proc. 6th ACM Conf. Computational Geometry 1990, 139–147.
- [15] W. P. Thurston, *Three-dimensional geometry and topology* Princeton University Lecture Notes, 1978.
- [16] F. Waldhausen, The word problem in fundamental groups of sufficiently large irreducible 3-manifolds, Annals of Math. (2) 88 1968 272–280.
- [17] D. J. A. Welsh, *Complexity: Knots, Colourings and Counting*, Cambridge University Press: Cambridge 1993.
- [18] D. J. A. Welsh, Knots and braids: some algorithmic questions, in: *Graph Structure Theory* (Seattle, WA 1991), Contemporary Math. Vol. 147, AMS: Providence 1993, pp. 109–123.

DEPARTMENT OF MATHEMATICS, UNIVERSITY OF CALIFORNIA, DAVIS CALIFORNIA 95616
E-mail address: `hass@math.ucdavis.edu`

DEPARTMENT OF COMPUTER SCIENCE, UNIVERSITY OF NORTH CAROLINA, CHAPEL HILL, NC
27514
E-mail address: `snoeyink@cs.unc.edu`

DEPARTMENT OF MATHEMATICS, UNIVERSITY OF CALIFORNIA, DAVIS CALIFORNIA 95616
E-mail address: `wpt@math.ucdavis.edu`